



ORIGINAL ARTICLE

Investigating key factors underlying neurodegeneration linked to alpha-synuclein spread

Cindy C. C. Pang^{1,2} | Maja H. Sørensen¹ | Krit Lee¹ | Kelvin C. Luk³ |
John Q. Trojanowski^{3†} | Virginia M. Y. Lee³ | Wendy Noble²  |
Raymond C. C. Chang^{1,4} 

¹Laboratory of Neurodegenerative Diseases, School of Biomedical Sciences, LKS Faculty of Medicine, The University of Hong Kong, Hong Kong SAR, China

²Institute of Psychiatry, Psychology and Neuroscience, Department of Basic and Clinical Neuroscience, King's College London, London, UK

³Center for Neurodegenerative Disease Research, Department of Pathology and Laboratory Medicine, Alzheimer's Disease Core Center, Institute on Aging, University of Pennsylvania Perelman School of Medicine, Philadelphia, Pennsylvania, USA

⁴State Key Laboratory of Brain and Cognitive Sciences, The University of Hong Kong, Pokfulam, Hong Kong SAR, China

Correspondence

Raymond Chuen-Chung Chang, School of Biomedical Sciences, LKS Faculty of Medicine, The University of Hong Kong, Rm. L4-49, Laboratory Block, Faculty of Medicine Building, 21 Sassoon Road, Pokfulam, Hong Kong SAR, China.
Email: rcchang@hku.hk

Wendy Noble, King's College London, Department of Basic and Clinical Neuroscience, Room 1.23 Maurice Wohl Clinical Neuroscience Institute, 5 Cutcombe Road, London SE5 8RX, UK.
Email: wendy.noble@kcl.ac.uk

Funding information

The study is supported by Innovative and Technology Fund (ITS/381/15) from Innovative and Technology Commission, Seed Funding for Basic Science Research (201910159221 and 201711159222) from The University of Hong Kong. CCCP and MHS are fully supported by Postgraduate Stipend from the Graduate School, LKS Faculty of Medicine and research fund from RCCC, The University of Hong Kong. CCCP is also supported by research funds from WN, King's College London, and the King's College London Alzheimer's Research UK Network Centre. JQT and VMYL were supported in this study in part by grants from the National Institutes of Health (AG10124, AG16573,

Abstract

Aims: It has long been considered that accumulation of pathological alpha-synuclein (aSyn) leads to synaptic/neuronal loss which then results in behavioural and cognitive dysfunction. To investigate this claim, we investigated effects downstream of aSyn preformed fibrils (PFFs) and 6-hydroxydopamine (6-OHDA), because aSyn PFFs induce spreading/accumulation of aSyn, and 6-OHDA rapidly causes local neuronal loss.

Methods: We injected mouse aSyn PFFs into the medial forebrain bundle (MFB) of Sprague–Dawley rats. We investigated spread of pathological aSyn, phosphorylation of aSyn and tau, oxidative stress, synaptic/neuronal loss and cognitive dysfunction 60, 90 and 120 days after injection. Similarly, we injected 6-OHDA into the MFB and examined the same parameters 1 and 3 weeks after injection.

Results: Following aSyn PFF injection, phosphorylated aSyn was found distant from the injection site in the hippocampus and frontal cortex. However, despite neuron loss being evident close to the site of injection in the substantia nigra at 120 days post injection, there were no other neurodegeneration-associated features associated with aSyn including synaptic loss. In contrast, 6-OHDA caused severe neuronal loss in the substantia nigra at 3 weeks post injection that was accompanied by phosphorylation of aSyn and tau, oxidative stress, loss of synaptic proteins, cognitive and motor dysfunction.

Conclusions: Our results demonstrate that spread/replication and slow accumulation of pathological aSyn may not be sufficient to induce neurodegenerative changes. In contrast, oxidative stress responses in addition to aSyn accumulation were associated

We dedicate this manuscript to the memory of Professor John Trojanowski as he passed away while the manuscript was being reviewed.

† In memoriam.

This is an open access article under the terms of the [Creative Commons Attribution](https://creativecommons.org/licenses/by/4.0/) License, which permits use, distribution and reproduction in any medium, provided the original work is properly cited.

© 2022 The Authors. *Neuropathology and Applied Neurobiology* published by John Wiley & Sons Ltd on behalf of British Neuropathological Society.

AG17586, R01AG021055, R01AG042444,
P50AG16573 and MH64045).

with other Parkinson's disease (PD)-associated abnormalities and cognitive dysfunction. Our results may be important when considering why only some PD patients develop dementia.

KEYWORDS

6-OHDA, alpha-synuclein, Parkinson's disease, oxidative stress, Tau

INTRODUCTION

Abnormal aggregation of beta-amyloid (A β), tau and aSyn are hallmark pathologies in several neurodegenerative disorders, and this trio of proteins has been postulated to act synergistically leading to exacerbated neurodegeneration, behavioural and cognitive impairments [1–4]. The accumulation and spread and/or templating of pathological proteins may be the first step of sequential neurodegenerative processes, which cause synaptic degeneration/neuronal loss (second step) and impairment of behaviour (e.g., motor or cognitive functions as the third step). Neuroinflammation may promote disease progression throughout this process [5]. We investigated the relationship between these events, with the aim of better understanding the neurodegenerative process involved in the emergence of cognitive dysfunction in models of Parkinson's disease (PD) that could give clues into the mechanisms underlying the conversion of PD to PD dementia (PDD).

PD is characterised by its well-known neuropathological hallmarks, that is, Lewy bodies (LBs) and Lewy neurites (LNs), that are composed primarily of misfolded aSyn. LBs contain β -sheet rich aSyn amyloid fibrils, frequently observed across all synucleinopathies [6, 7]. The presence of LBs and LNs also correlates closely with PDD. Approximately 80% of PD patients develop PDD or other cognitive dysfunction 10–15 years after the onset of PD, which leads to the rapid demise of these patients [8]. Unlike AD, where memory loss is predominant, executive functions such as attention, inhibition and visuospatial impairment can be more common than memory loss in PDD [9]. Regions thought to be associated with executive dysfunction and visuospatial impairment include the frontal cortex and hippocampus [10–12].

The cell-to-cell transmission and/or replication of misfolded aSyn are considered key mechanisms in the progression of PD [13, 14]. Dementia in synucleinopathies is thought to be due to aSyn-linked abnormalities at cortical and hippocampal synapses [15]. Therefore, studying the temporal emergence of aSyn abnormalities allows us to understand the relationship between abnormal forms of aSyn, perturbation of synapses and neuronal loss and cognitive dysfunction.

Although the accumulation of misfolded aSyn is considered by many as key to the pathogenesis of PD and PDD, other mediators such as oxidative/nitrative stress have also been reported to play a role in the neurodegeneration cascade. A bi-directional relationship between aSyn and oxidative/nitrative stress has been observed in cell culture studies, where each factor can exacerbate the detrimental effects of the other [16–18]. An increase in oxidative stress markers was also noted in post-mortem PD brains compared with controls.

Key points

- Injection of preformed fibril of α -synuclein into the medial forebrain bundles induced phosphorylated α -synuclein in the hippocampus and frontal cortex but no obvious neurodegeneration in these two brain regions in 120 days.
- Injection of 6-hydroxydopamine in the same site induced free radicals, massive neuronal loss in the substantia nigra and phosphorylated α -synuclein in the hippocampus and frontal cortex with increased oxidative stress in 3 weeks.
- Free radicals seem to be an important factor inducing phosphorylation of α -synuclein in other brain regions distance from the injection site.

These markers include 4-hydroxyl-2-nonenal (HNE), a by-product of lipid peroxidation [19, 20], and 8-hydroxy-deoxyguanosine (8OHG), a DNA and RNA oxidation product [21, 22]. Furthermore, the reactive nitrogen species nitrotyrosine is detected in LB's within melanin containing substantia nigra (SN) neurons and other neurons containing amorphous deposits associated with both degenerating and intact neurons, suggesting that oxidative stress is induced in PD [23, 24].

Oxidative stress is also widely believed to be a common mechanism that leads to cellular dysfunction and neurodegeneration in both genetic and idiopathic types of PD [25]. Intracerebral injections of 6-hydroxydopamine (6-OHDA) in experimental models of PD trigger oxidative stress responses resulting in the loss of dopaminergic neurons in the SN and dorsal striatum (ST). Dying neurons then produce more reactive oxygen species (ROS) or reactive nitrogen species (RNS) that promote accumulation of pathological proteins [26].

In rodents, injection of aSyn preformed fibrils (PFFs) in the brain induces neuronal accumulation of phosphorylated aSyn which subsequently spreads to interconnected neurons. This accumulation of aSyn is proposed to induce synaptic disruption, neuron loss and cognitive behavioural phenotypes [27–29]. However, it takes several months after aSyn brain injections before neurodegeneration is apparent [30–32]. In contrast, injection of the parkinsonian mimetic 6-OHDA, into the medial forebrain bundle (MFB) region, triggers marked neuronal loss within three weeks [33].

These two experimental models allowed us to investigate the relationship between aSyn spread and neurodegeneration in regions distinct from the site of injection. To achieve this objective, either

aSyn PFFs or 6-OHDA were injected into the MFB of Sprague–Dawley (SD) rats, as this bundle of fibres contains axons that project to the ST, frontal cortex and hippocampus [34]. The MFB is an intricate structure composed of a descending and ascending system of fibres that connect medial and basal forebrain structures [34–36]. Ascending axons from dopaminergic, serotonergic and noradrenergic neurons located in the lower brain stem also pass through the MFB [34]. The MFB is best known for its connectivity between the ST and SN, making it a popular injection site for investigating PD-like features in animal models. In rats, the MFB has both output and input projections to and from a diverse range of regions including the locus coeruleus, neocortex, hypothalamus, septum, thalamus and cerebellum [34, 37]. Injection of material into the MFB therefore allows us to study the effects on projection regions such as the frontal cortex that control executive function. Both groups of rats were subjected to behavioural tests to assess cognitive and motor dysfunction, followed by morphological immunohistochemical methods and biochemical analysis to detect specific disease related proteins and abnormal synaptic proteins.

Our results show that neurodegeneration and the onset of cognitive dysfunction do not temporally accompany the progressive accumulation of aSyn in regions distal to the site of PFF injection, including the frontal cortex and hippocampus. However, substantial neuronal loss induced by 6-OHDA was contemporaneous with aSyn accumulation, synapse loss and cognitive decline. Unlike following PFF injection, a marked oxidative stress response was observed in the 6-OHDA model. We speculate that oxidative stress exerted directly by 6-OHDA induces marked neuron loss, with degenerating neurons producing oxidative/nitrative stress environments that facilitates the accumulation of pathological aSyn leading to synapse loss, neurodegeneration and cognitive deficits. Our results provide insights into the mechanisms of PD pathogenesis that may be relevant for determining the rate of conversion of PD to PDD.

MATERIALS AND METHODS

Stereotactic injections into the rat MFB

Adult 230–250 g wild-type male SD rats were obtained from the Center for Comparative Medicine Research, LKS Faculty of Medicine, which is accredited by the Association for Assessment and Accreditation of Laboratory Animal Care (AAALAC). All animal studies were approved by the University of Hong Kong (HKU) and performed in accordance with the Committee on the use of Live animals in teaching and research (CULATR regulations), in which the guidelines of the National Centre for the Replacement, Refinement and Reduction of Animals in Research, UK, and NIH Guidelines for Survival Rodent Surgery, USA are followed.

The rats had constant access to food and water and were housed 2–3 per cage under a 12-h light/12-h dark cycle. On the day of surgery, PFFs prepared from recombinant mouse aSyn were thawed and sonicated as previously described [38]. Rats anaesthetised with

ketamine hydrochloride (100 mg/kg, intraperitoneally) (i.p.) and xylazine (10 mg/kg, i.p.) were immobilised on a stereotaxic frame (Narishige Scientific Instruments Lab, Japan), adapted from Zhang et al. [39]. Rats were aseptically injected unilaterally in the MFB: AP = –4.0, ML = –1.2 and DV = +7.5 (below dura), from coordinates adapted from Shah et al. and Torres et al. [33, 40] relative to the bregma, either with recombinant aSyn PFFs (6 µg/µl; 30 µg), 6-OHDA (3 µg/µl; 12 µg) or sterile phosphate-buffered saline (PBS), 5 µl for the aSyn PFFs group or 4 µl for the 6-OHDA group, using a 10 µl syringe, gauge 33 (Hamilton, NV) at a rate of 0.5 µl/min. Post-surgery, rats received Metacam® (Meloxicam, Boehringer, Ingelheim, Germany) at 1 mg/kg into their drinking water as analgesia and were monitored regularly as described elsewhere [33].

Behavioural testing

Smart 3.0 software (Panlab, USA) was used when applicable in conjunction with video camera recordings to allow the tracking of animal movement during behavioural tests and subsequent analyses. Unless stated otherwise, behavioural experiments were not conducted consecutively within a 2-day period to ensure that rats had enough rest in between tests. Rats were also habituated inside the behaviour room for 30 min prior to testing. Rats injected with aSyn PFFs and control material were from separate cohorts from those injected with 6-OHDA and their controls. Rats went through the battery of tests in the same order, that is, open field testing followed by asymmetric cylinder test and concluding with testing in the Morris water maze (MWM).

Locomotion and anxiety-related activity were assessed using open field testing according to previously published protocols [41]. Rats were examined for asymmetry of forelimb use by the cylinder test as previously described [42]. Analysis of drug-induced rotations was recorded digitally on a camcorder for 30 min using a previously described protocol adapted from Jerussi and Glick [43]. To measure visuospatial related cognitive impairment, the escape latency and number of platform crossings were recorded using the MWM task. The MWM was used here as previously described [44–46].

Collection of tissue

At 60, 90 or 120 d.p.i. of aSyn PFF, in accordance with previous studies [30, 32], and 1 or 3 weeks post-injection (w.p.i.) of 6-OHDA [33], rats were anaesthetized with i.p. injections of pentobarbitone at 120 mg/kg followed by transcranial perfusion with cold 0.9% saline and 4% paraformaldehyde (PFA). Brains were dissected and post-fixed overnight in 4% PFA for histopathology or were snap frozen on dry ice and stored at –80°C for biochemistry, as previously described [33, 47].

Human brain tissue

Formalin-fixed, paraffin-embedded brain sections at 7 µm thick from neuropathologically assessed human brain with tau pathology at Braak

stage VI (AD; temporal cortex) were obtained as previously described in from Brains for Dementia Research/The London Neurodegenerative Disease Brain Bank, King's College London, UK [48].

Immunohistochemical staining

Fixed rat brain tissues were embedded into paraffin blocks, sectioned at 7 μ m and immunolabelled as previously described using antibodies against pSer129 aSyn (81A, CNDR 1: 10,000), AT8 (Thermo scientific #MN1020, 1:50), PHF1 (Peter Davies 1:100), tau pS404 (Thermo scientific #44-758G, 1:20), 8-hydroxy-2-deoxyguanosine (Abcam #ab62623, 1:150) and anti-nitrotyrosine antibody (Thermo scientific #A-21285, 1:500) [47].

Western blot

Western blot was performed following determination of sample protein concentration using a BCA assay kit (Pierce, Thermo; Rockford, IL, USA). Membranes were probed with antibodies against glial fibrillary acidic protein (DAKO/Agilent Technologies, 1:1000), synaptophysin (Santa Cruz, #sc-17750, 1:1000), synaptotagmin (Abcam, #ab51164 1:1000), PSD-95 (CST, #3450, 1:1000), NR2B (Millipore, #06-600, 1:1000) and β -actin (Abcam, #ab8227, 1:5000).

Quantification and statistical analysis

All statistical analyses were performed on Prism V6.0 (GraphPad Software, Inc., USA). Figure legends report the statistical analysis performed, the number of rats (*n*) analysed in each experiment and the *p* values. The level of significance was set at $p < 0.05$. All data are presented as mean \pm SEM.

RESULTS

aSyn PFFs induced accumulation of phosphorylated aSyn but not phosphorylation of tau in the frontal cortex and hippocampus

The spread and/or replication of phosphorylated aSyn after aSyn PFF injections into various anatomical regions has been widely demonstrated [28, 29, 31, 32, 49]. Here, we show that injection of aSyn PFFs into the MFB of SD rats (Figure S1) resulted in phosphorylated aSyn immunoreactivity being detected in the frontal cortex, hippocampus, ST and SN (Figure 1A) from 60 d.p.i. Phosphorylated aSyn was detected in both hemispheres, with the number of positively labelled cells peaking at 90 d.p.i. as indicated by the load of brown circles, each of which represents a positively immunolabelled neuron (Figure 1B). No phosphorylated aSyn was found in the brain of PBS-injected controls. Quantification of the total positive immunolabelled

phosphorylated aSyn count within each region for all time points is shown in Figure S2. Although immunoreactivity for phosphorylated aSyn can often be indicative of aSyn aggregates, we further investigated the solubility of aSyn in frontal cortex samples taken at 90 d. p.i. on the basis of its solubility in increasingly stringent detergents, as has been performed previously [7]. We were unable to detect any aSyn that was insoluble in sarkosyl, with the majority of aSyn being isolated in high salt, high salt triton-x and sarkosyl-soluble fractions (Figure S3). This suggests that the aSyn we detected by immunohistochemistry (IHC) may not be bona fide aggregates, at least on the basis of their solubility in these detergents. It is possible, however, that the relative sparsity of aSyn inclusions prevents us from readily detecting aggregates in whole tissue homogenates.

Although there is abundant evidence of a synergistic relationship between aSyn and tau in LB disorders (LBDs) such as PD [3, 50, 51], aSyn PFFs per se rarely lead to any change in tau [52], with only specific strains capable of inducing tau phosphorylation [53, 54]. We performed immunohistochemical staining for tau phosphorylated at S404 and pS396/404 (PHF1). No substantial immunoreactivity was noted for any of these epitopes within the frontal cortex or hippocampus of either aSyn PFF or sham-injected groups at 90 d.p.i. (Figure S4). With the use of a similar approach to that described for aSyn, we also found no apparent differences in the solubility of tau between control- and PFF-injected rats (Figure S5).

aSyn did not induce any further neurodegeneration-associated changes in the frontal cortex or hippocampus, although significant neuronal loss was observed in the SN from 120 d.p.i.

To determine if any common features of PD-like neurodegeneration resulted from aSyn PFF injection into rat MFB, we examined synaptic protein levels. It has previously been reported that aSyn PFFs are able to compromise synaptic activity and enhance synapse loss in cultured neurons [55]. Western blots showed no significant alteration in the levels of the post-synaptic proteins PSD-95 and NR2B or the presynaptic proteins synaptotagmin and synaptophysin in either frontal cortex or hippocampus of aSyn PFF-injected rats at 90 d.p.i. relative to control (Figure S6).

Previous work has demonstrated progressive dopaminergic neuron loss within the SN upon administration of aSyn PFFs [28, 32, 56, 57]. Of the three time points being investigated in this study, a statistically significant TH cell loss was noted at 120 d.p.i. (Figure 1C,D) but not at earlier time points (data not shown). Despite this neuronal loss, there was no evidence of other neurodegenerative changes in these samples or neuronal loss in other brain regions by 120 d.p.i.

The Parkinsonian mimetic 6-OHDA induced phosphorylation of aSyn and tau in the frontal cortex and hippocampus

Our results showed that the appearance of pathological aSyn in regions distant from the MFB requires extended time (over 120 d.p.i.), despite neuronal loss in the SN being detected at 120 d.p.i. To further

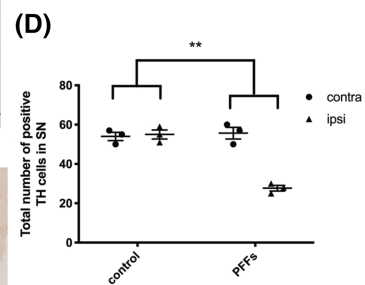
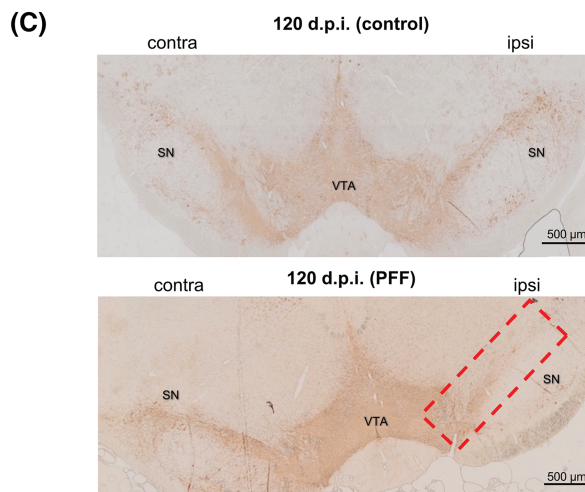
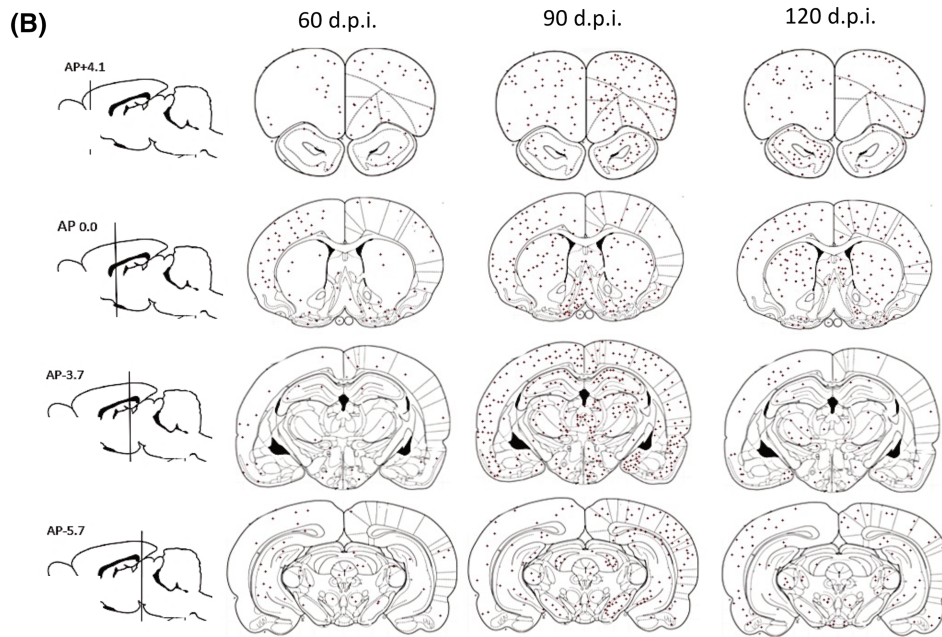
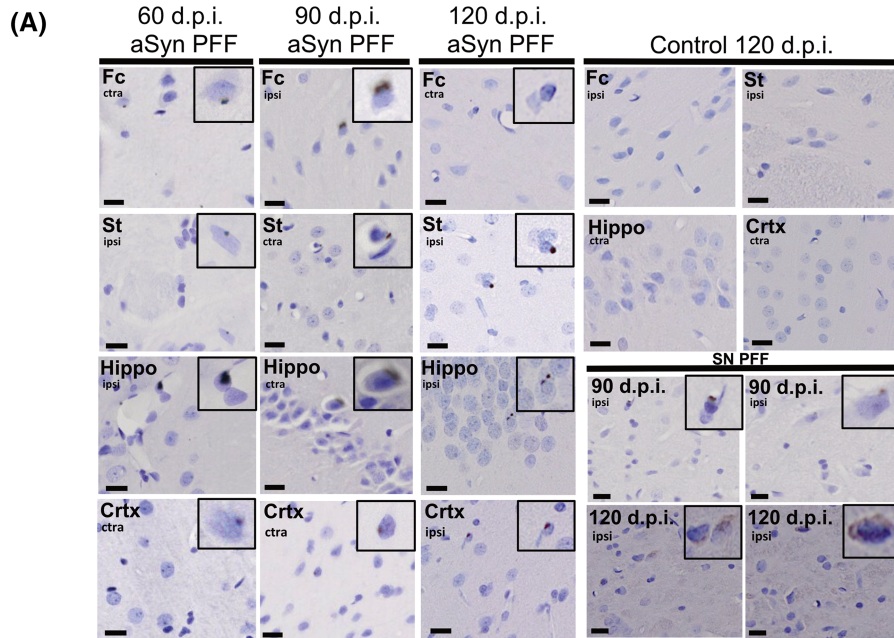


FIGURE 1 Phosphorylated alpha-synuclein (aSyn) slowly accumulates in regions distant from the preformed fibril (PFF) injection site. (A) Using a stereological approach, a 1 in 20 sequence of 7 μm coronal sections was taken throughout the entire brain (both contralateral and ipsilateral hemispheres) of animals injected with aSyn PFFs for 60, 90 and 120 d.p.i. or control (vehicle) for 120 d.p.i. Representative images are shown. Sections were immunolabelled with an antibody against aSyn phosphorylated at Ser129 and counterstained with haematoxylin to label nuclei. Phosphorylated aSyn inclusions appeared as faint cytoplasmic and denser perinuclear inclusions in the frontal cortex (Fc), striatum (St), hippocampus (Hippo), cortex (Ctx) and substantia nigra (SN). Control animals did not show any positive labelling. Scale bars = 10 μm , $n = 3$. (B) The total number of positively immunolabelled cells in three animals from each PFF-injected group was counted and the positions marked on coronal brain tracings. Cells positive for phosphorylated aSyn were observed in many regions including those directly and indirectly connected to the medial forebrain bundle (MFB) and appeared to peak at 90 d.p.i. The red circle indicates the site of injection (MFB). Regions proximal to the injection site appeared to show the most abundant phosphorylated aSyn positive cells; (C) 7 μm coronal sections from control and PFF-injected rats at 120 d.p.i. were immunolabelled using an antibody raised against tyrosine hydroxylase (TH). Representative images are shown. Red box identifies region of interest used for quantification. (D) Quantification of TH cell count for 120 d.p.i. tissues. To detect differences in cell number between PFF and control groups, an unpaired t test was used. This showed a statistically significant reduction in TH cell number in the PFF group. $**p < 0.01$. Data shown are mean \pm SEM, $n = 3$.

understand the neurodegenerative processes, we injected the Parkinsonian mimetic 6-OHDA into the MFB of another cohort of rats. Three weeks post-injection, we performed immunohistochemical staining on brain sections from 6-OHDA-injected rats and their controls. We observed some phosphorylated aSyn-positive cells in the frontal cortex and hippocampus of 6-OHDA-injected rats but not in PBS-injected controls (Figure 2A). Individual immunoreactive neurons in the frontal cortex, ST, hippocampus and other cortical areas are represented in Figure 2B. The total number of positively immunolabelled phosphorylated aSyn cells within each of those regions is shown in Figure S7. aSyn immunoreactivity was not observed in these regions at 1 week post-injection (Figure S8). These findings show that 6-OHDA can induce modest phosphorylation of aSyn in brain regions distal from the site injection in a rapid time frame (3 weeks).

We also examined tau phosphorylation in the frontal cortex and hippocampus. The phosphorylation and synaptic mislocalisation of tau are biological determinants of dementia in AD [58], and modified tau has been reported in PD and PDD brains [3, 4, 59]. Following 6-OHDA injections, there was increased tau phosphorylation at S404, S396 and S396/404 (PHF1), sites known to be aberrantly phosphorylated in AD brain [60]. Phosphorylation of tau at S404 was found at basal levels in control human brain and is increased in AD [61] (Figure 3A). Accordingly, pS404 and pS396 immunoreactivity was apparent in CA1 and particularly in CA3 of both control and 6-OHDA-injected rats (Figures 3B and 4A–C), and labelling intensity was significantly increased in hippocampal sub-fields in the 6-OHDA-injected group (Figure 3C,D). The MFB has indirect projections to the frontal cortex, and this area also displayed immunoreactivity for phosphorylated tau at pS404, particularly in 6-OHDA-injected rats, in both contralateral and ipsilateral hemisphere (Figure 3E,F). We also observed pS396 immunolabelling on both contralateral and ipsilateral sides of the frontal cortex, with an apparent increase of pS396 immunoreactivity in the 6-OHDA-injected group compared to controls (Figure 4D,E). Immunoreactivity against the PHF1 antibody requires tau phosphorylation at both Ser396 and Ser404 and is characteristic of abnormally modified tau in disease [61] (Figure S9A). Faint PHF1 immunoreactivity was observed in the hippocampus of 6-OHDA-injected rats and was largely absent from control rat hippocampus

(Figure S9B–E). PHF1 immunoreactivity was mostly absent within the frontal cortex of both control and 6-OHDA-injected rats (Figure S9F,G). These results show that 6-OHDA induces phosphorylation of some tau epitopes that allow tau pathology to be established in the frontal cortex and hippocampus, regions distal to the injection site.

6-OHDA induced loss of the post-synaptic protein PSD-95 in the frontal cortex and substantial neuronal loss in the SN

Synaptic deficits underlie cognitive decline and dementia in neurodegenerative diseases [15, 62, 63]. Thus, we examined if 6-OHDA affects the levels of synaptic proteins. Western blot of frontal cortex lysates showed a significant reduction of the post-synaptic protein PSD-95 bilaterally (Figure 5A,C). Reduction in PSD-95 was, however, not noted within the hippocampus (Figure 5B,D) of 6-OHDA-injected rats. There were no significant changes in the amounts of NR2B or the pre-synaptic markers synaptotagmin and synaptophysin in the frontal cortex or hippocampus at 3 weeks post-injection (Figure S10).

We also examined neuronal loss in the SN as this is a defining feature of PD and PDD. 6-OHDA-injected rats showed substantial loss of TH-positive neurons in the ipsilateral SN at 3 weeks post-injection (Figure 6A). A statistically significant reduction in TH immunolabelling was also noted between the ipsilateral hemisphere of control rats and both hemispheres of 6-OHDA-injected rats after 3 weeks (Figure 6B). Because dying neurons release several toxic factors that may be transmitted to other regions of the brain along projections, SN neuron loss may influence the rapid neurodegenerative changes we found in the frontal cortex and hippocampus.

Oxidative and nitrate stress was apparent in the frontal cortex and hippocampus following 6-OHDA injection into the MFB

One type of toxic factor released from dying neurons are free radicals, which trigger both oxidative stress and nitrate stress. Therefore, we

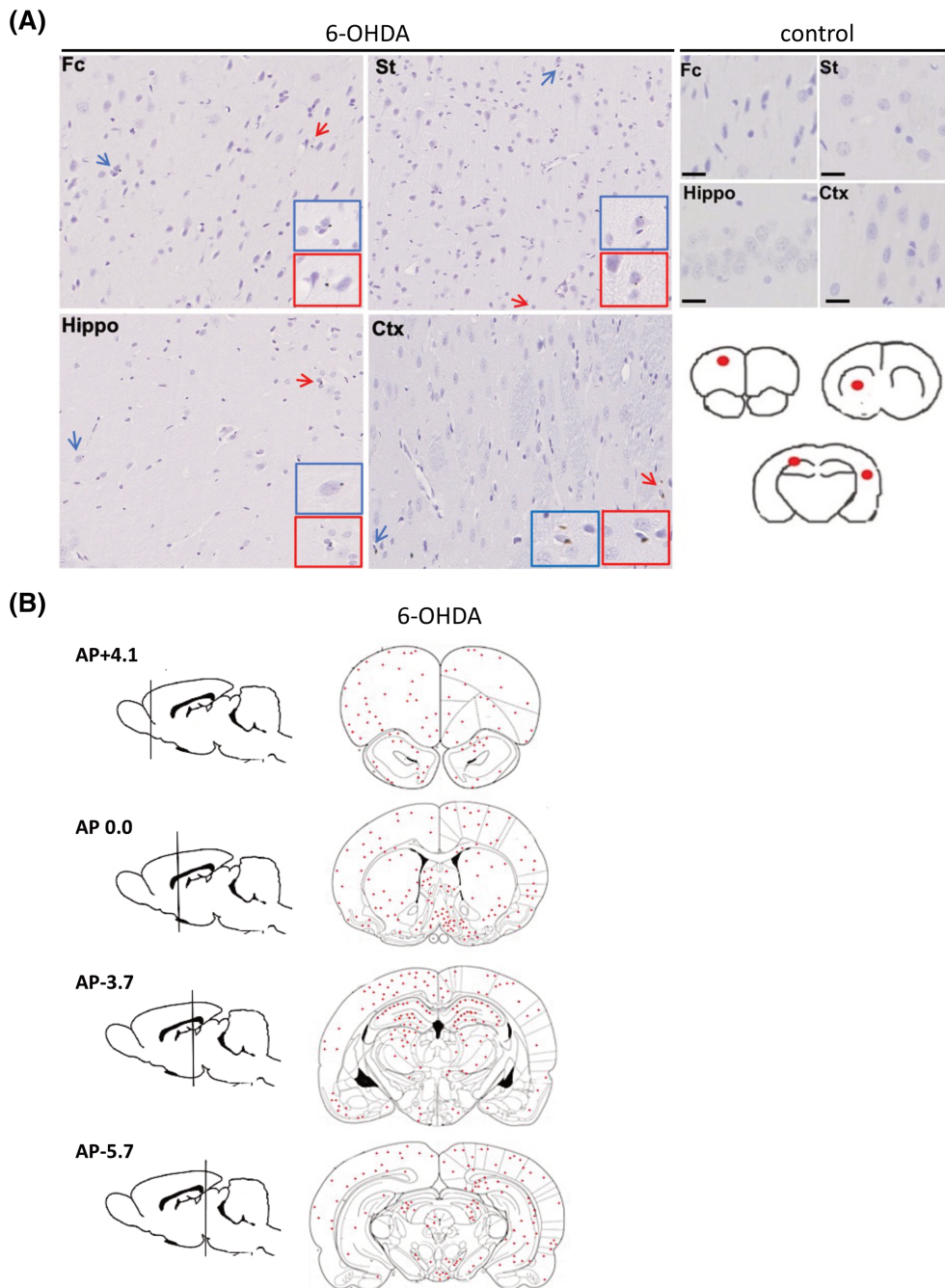


FIGURE 2 Phosphorylated alpha-synuclein (aSyn) rapidly accumulates in regions distant from the 6-OHDA injection site. (A) Immunohistochemistry was performed on 7 μ m thick brain tissues from rats unilaterally injected with phosphate-buffered saline (PBS) (control) or 6-OHDA into the medial forebrain bundle (MFB). An antibody raised against phosphorylated aSyn at serine 129 (81A) was used to label cells containing phosphorylated aSyn. Control rats (top right panel) did not show any 81A immunoreactivity, whereas cells showed faint positive labelling for phosphorylated aSyn in Fc, St, Hippo and Crtx in response to 6OHDA (middle panel). Red scale bar 20 μ m, black scale bar, 5 μ m, $n = 3$. Blue and red arrows indicate cells immunoreactive to the phosphorylated aSyn antibody, with coloured insets showed higher magnification images of these cells. Images are from representative rodents. Fc = frontal cortex, St = striatum, Hippo = hippocampus and Crtx = cortex. Red circles on brain traces (bottom right panel) show the Fc, striatum, hippocampus and cortical areas from which sections were obtained and immunolabelled. (B) The total number of positively immunolabelled cells in three animals from the 6-OHDA-injected group was counted and the positions marked on coronal brain tracings. Cells positive for phosphorylated aSyn were observed in many regions including those directly and indirectly connected to the MFB.

examined oxidative stress in the frontal cortex and the hippocampus 3 weeks post-injection by immunostaining with an antibody against 8OHG, and nitritive stress was assessed by immunoreactivity to

anti-nitrotyrosine antibody. Increased oxidative stress responses in the frontal cortex were confirmed using an antibody specific to 8OHG (Figure 7A,C) within the 6-OHDA-injected group compared with

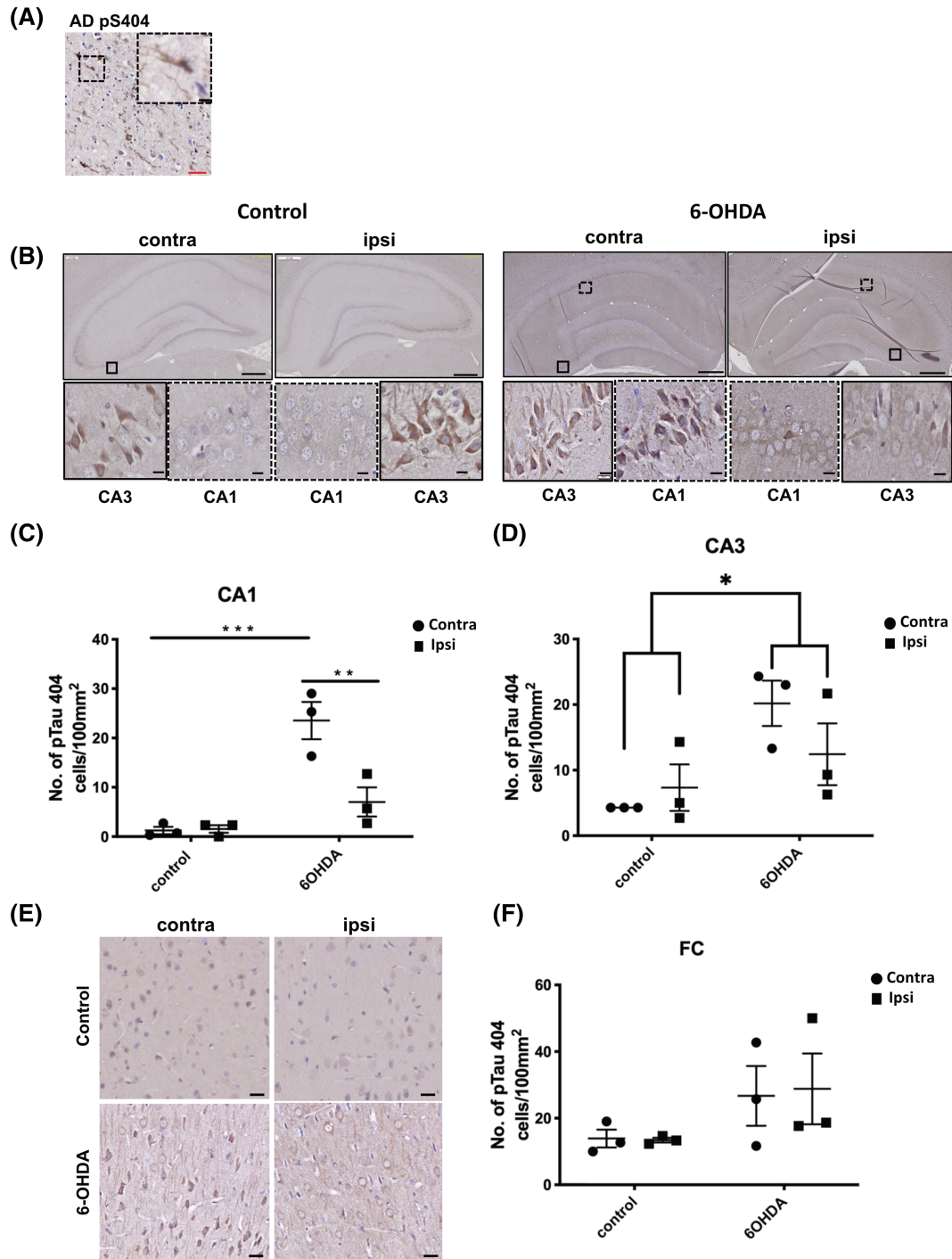


FIGURE 3 (A) Tau phosphorylated at Ser404 rapidly accumulates in regions distant from the 6-OHDA injection site. Immunohistochemical staining was performed on 7 μ m paraffin embedded sections from the temporal cortex of a post-mortem Alzheimer's disease (AD) brain using an antibody against pTau404. Inset shows higher magnification of immunoreactive neurons. For rat brain, 7 μ m paraffin embedded sections were labelled with the same antibody against pTau404. (B) Representative images of pTau404 immunolabelling at 3 weeks post injection. Sections were counterstained with haematoxylin. Both control and 6-OHDA-injected animals showed labelling of pTau404 in CA3. pTau404 labelling was also apparent in CA1 of 6-OHDA animals but not control animals. Bar charts in show quantification of the number of pTau404 +ve cells in (C) CA1 and (D) CA3. (E) Representative images of pTau404 immunolabelling in frontal cortex (Fc). Sections were counterstained with haematoxylin. Bar chart in (F) shows the number of pTau404 +ve cells in frontal cortex. Scale bars in main images are 500 μ m, and 5 μ m scale bars are used in insets. Unpaired *t* tests were used to determine differences in the number of immunoreactive cells between control and 6-OHDA groups for either the contralateral or ipsilateral hemisphere and demonstrated a statistically significant increase in pTau404-immunoreactive cells in the CA1 and CA3. No differences were found for the Fc region. **p* < 0.05, ****p* < 0.001. Data shown are mean \pm SEM, *n* = 3.

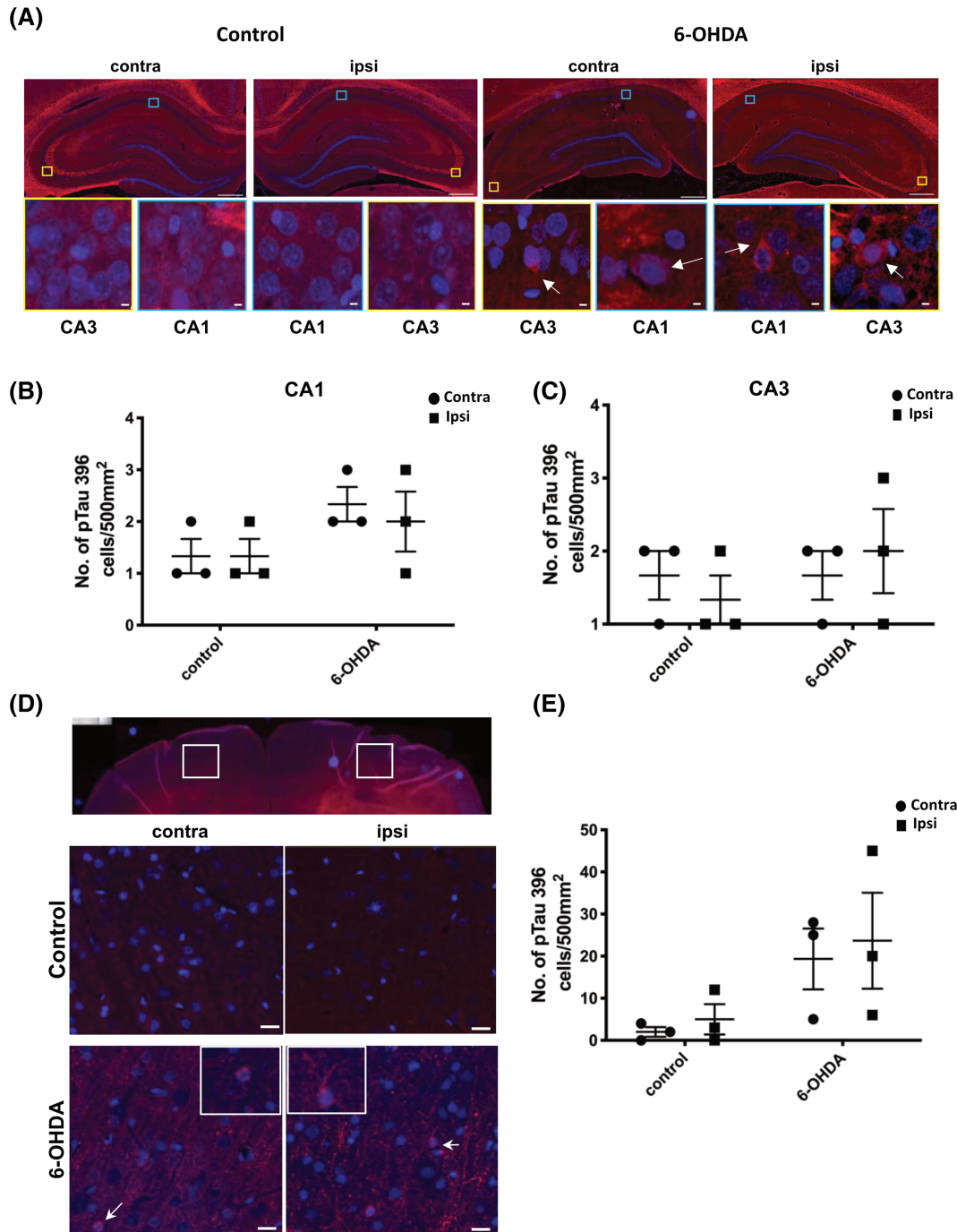


FIGURE 4 Cytoplasmic inclusions of tau phosphorylated at Ser396 are apparent following 6-OHDA injection into the medial forebrain bundle (MFB). (A) Representative immunofluorescence labelling of pTau396 in frontal cortex areas shown in low magnification images with white boxes, at 3 weeks post injection. DAPI (blue) used to stain nuclei. Control rat brain showed some background labelling, but unlike 6-OHDA-treated rats, little cytoplasmic pTau396 immunoreactivity was observed. Yellow and blue boxes indicate regions of CA3 and CA1, respectively, that are shown at higher magnification in insets. White arrows indicate specific areas of positive tau immunoreactivity in 6-OHDA-injected rat tissues. Scale bars in the main images are 500 μm , and 5 μm scale bars are used in the insets. Graphs show the number of pTau396 positive cells per mm^2 in the contralateral (contra) and ipsilateral (ipsi) hemispheres for (B) CA1 and (C) CA3. (D) Representative images of pTau396 immunolabelling in the frontal cortex (Fc). White arrows indicate area shown at higher magnification in insets. Scale bar 20 μm . (E) Quantification of the number of pTau396 positive cells in Fc. Unpaired *t* tests were used to determine differences in the number of immunoreactive cells between control and 6-OHDA groups for either the contralateral or ipsilateral hemisphere and did not indicate any statistical significance. Data shown are mean \pm SEM, *n* = 3.

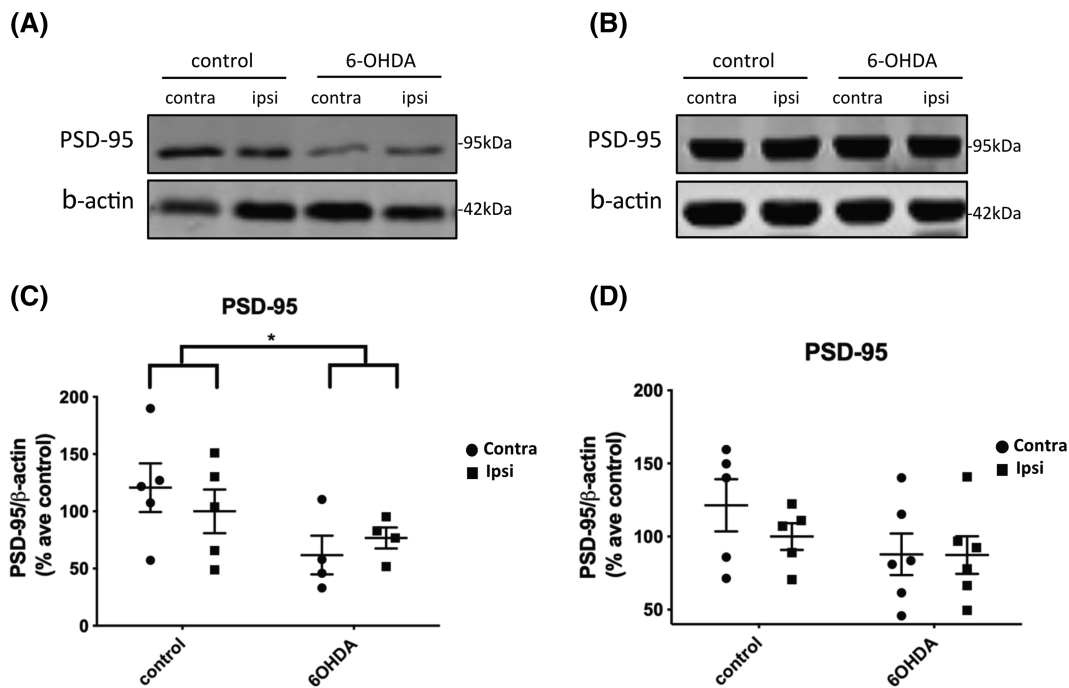


FIGURE 5 6-OHDA injection caused a loss of PSD-95 in the frontal cortex but not hippocampus. (A) Immunoblots of post-synaptic density protein-95 (PSD-95) in the high salt fraction of frontal cortex from 6-OHDA- and control-injected rats, 3 weeks post-injection. (A) Representative immunoblots from (A) frontal cortex and (B) hippocampus, probed with an antibody against the post-synaptic marker, PSD-95 (95 kDa). β-Actin was used as a loading control (42 kDa). (C) The dot plot shows a marked reduction in the amount of PSD-95 relative to β-actin in frontal cortex of 6-OHDA-injected rats relative to controls. Control, $n = 5$, preformed fibril (PFF), $n = 4$. (D) The dot plot shows no significant difference as a result of treatment or between hemispheres in the hippocampus, control, $n = 5$, PFF, $n = 6$. Unpaired t tests were used to determine differences in the amount of PSD-95 between control and 6-OHDA groups for either the contralateral or ipsilateral hemisphere and showed a significant effect of treatment. $*p < 0.05$. Data are mean \pm SEM presented as % average control where control is the ipsilateral hemisphere of control-injected rats.

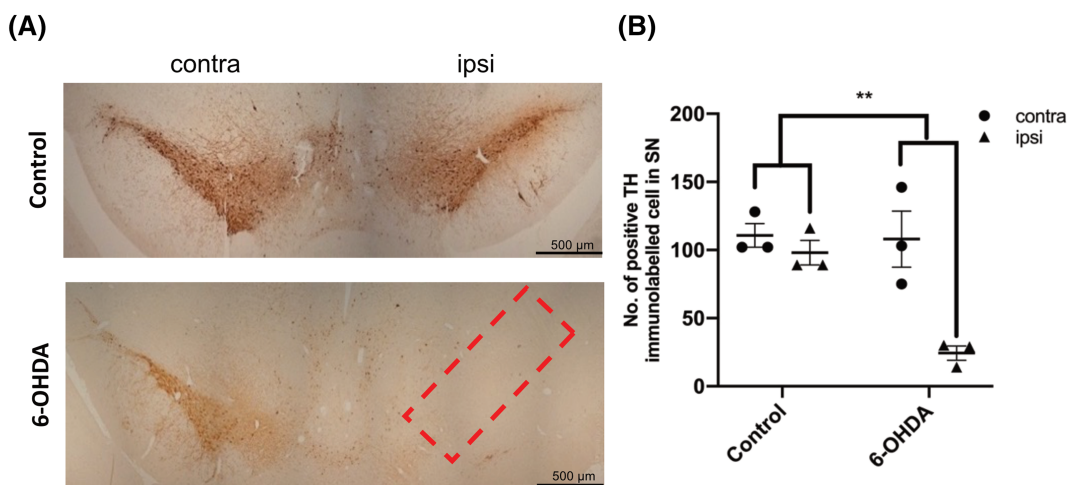


FIGURE 6 6-OHDA caused an ipsilateral loss of TH neurons in the substantia nigra 3 weeks after injection; (A) 7 μm sections from control and 6-OHDA-injected rats, 3 weeks post-injection, were immunolabelled using an antibody raised against TH. 6-OHDA-injected animals demonstrated an ipsilateral loss of TH +ve cells in the substantia nigra compared with control animals. Red box indicates the region of interest from which TH positive cells were counted. (B) Graph shows quantification of the number of TH positive cells in control and 6-OHDA animals, for both contralateral and ipsilateral hemispheres. Unpaired t tests were used to determine differences in cell count between control and 6-OHDA groups for either the contralateral or ipsilateral hemisphere and demonstrated a substantial reduction in TH positive cells within the ipsilateral hemisphere of 6-OHDA rats compared with control. $**p < 0.01$. Data are mean \pm SEM, $n = 3$.

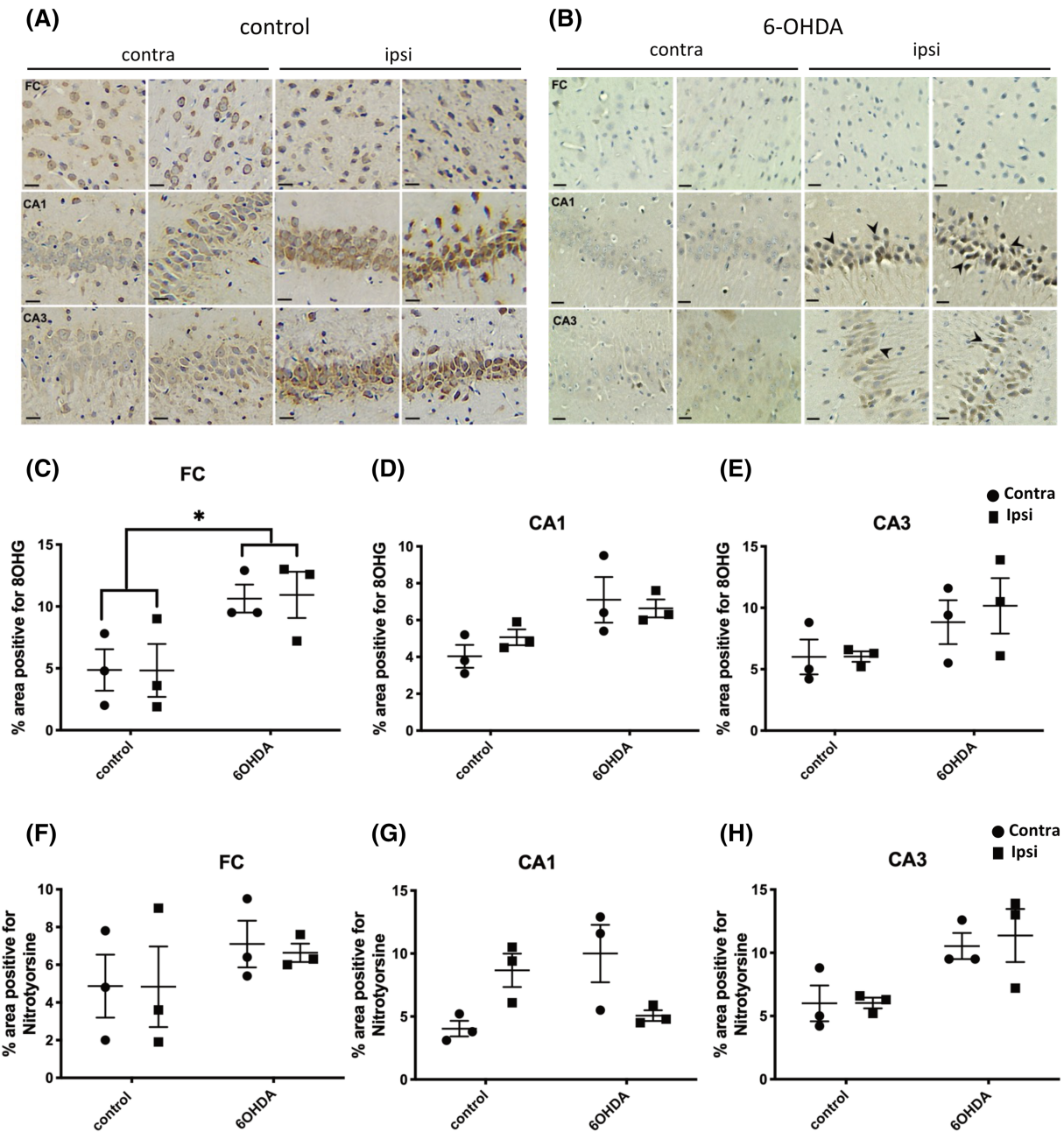


FIGURE 7 6-OHDA injection induced a widespread oxidative stress response; 7 μ m sections from control and 6-OHDA-injected rats, 3 weeks post-injection, were immunolabelled using antibodies raised against (A) anti-8-hydroxyguanosine (8OHG) to detect damage in DNA/RNA and (B) nitrotyrosine to indicate oxidative damage. Regions of the brain shown include frontal cortex and hippocampal subfields, CA1 and CA3, both contralateral (contra) and ipsilateral (ipsi) hemispheres. Scale bar 20 μ m. Graph shows quantification of the % area positive for 8OHG in (C) frontal cortex (Fc), (D) CA1 and (E) CA3, and for nitrotyrosine in (F) Fc, (G) CA1 and (H) CA3. Unpaired *t* tests were used to determine differences in immunoreactivity between control and 6-OHDA groups for either the contralateral or ipsilateral hemisphere and showed a statistically significant increase in 8OHG in the Fc. No other differences between groups were found. **p* < 0.05. Data are mean \pm SEM, *n* = 3.

control rats. Although the hippocampal subfields CA1 and CA3 also demonstrated an apparent increase in immunolabelling, it was not significant (Figure 7D,E). We found no significant increase in the percentage of 8OHG-positive cells in the frontal cortex, hippocampal CA1 or CA3 regions of aSyn PFF rats at 90 d.p.i (Figure S11B-D).

With the use of anti-nitrotyrosine antibodies (Figure 7B), we also noted a non-significant increase in nitrotyrosine-positive cells within the frontal cortex and hippocampal regions in 6-OHDA-injected rat brains when compared with control brains (Figure 7F-H). Similar to the results from 8OHG immunolabelling, aSyn PFFs rats did not show

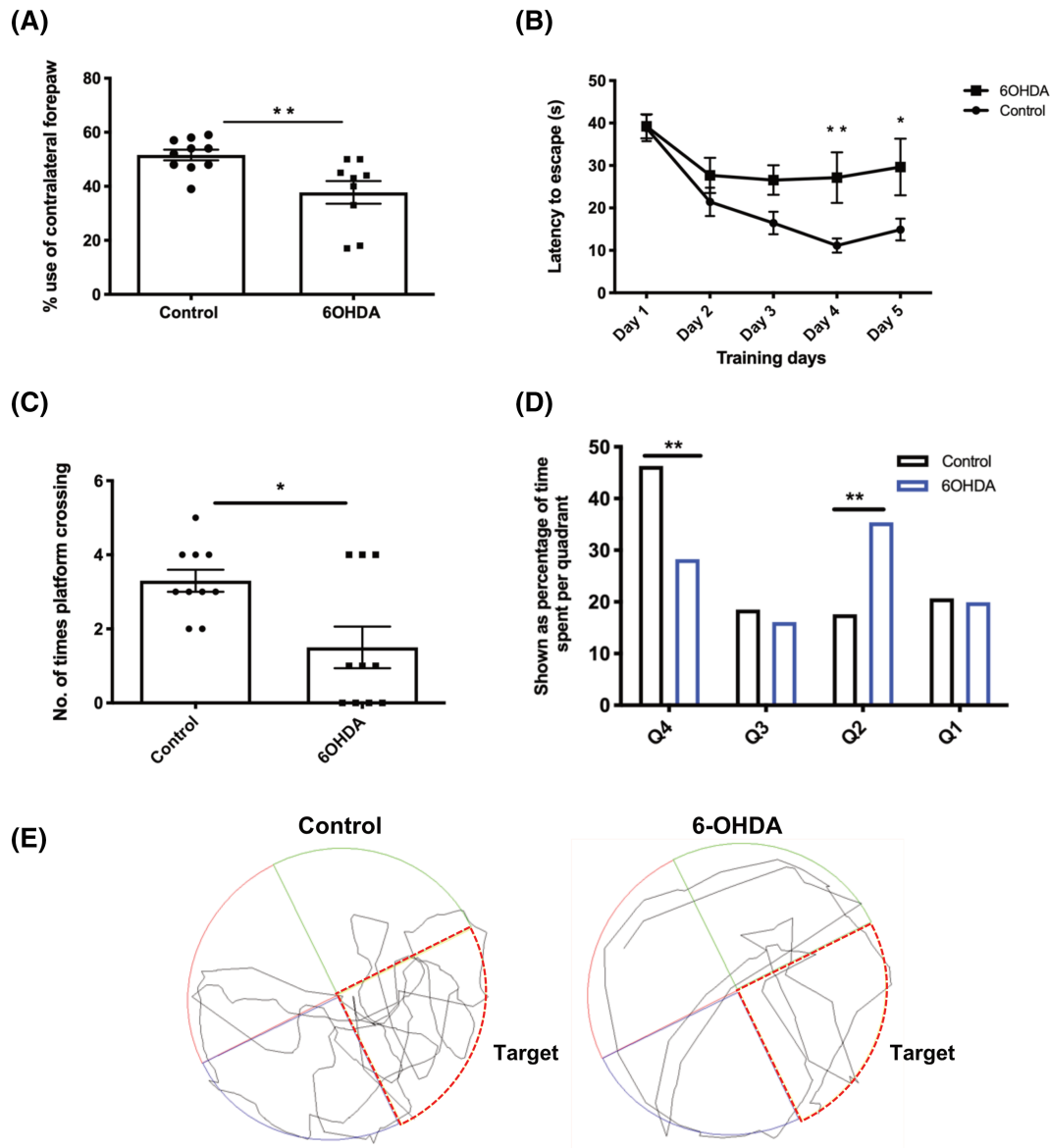


FIGURE 8 6-OHDA injection into rat medial forebrain bundle (MFB) induces motor and cognitive impairments. (A) The graph shows that 6-OHDA-injected animals show a contralateral forepaw impairment, with significantly reduced use of the contralateral forepaw compared with control animals during the asymmetric cylinder test, signifying a fine motor deficit. Data are mean \pm SEM, control, $n = 10$, 6-OHDA, $n = 9$. ** $p < 0.01$, statistical test used, unpaired t test. (B) Graph shows the learning curve during training Days 1–5. 6-OHDA-injected rats showed a learning deficit throughout the task compared with control animals where there was a reduction in escape latency from the initial training day. 6-OHDA-injected rats took significantly longer than control rats to escape the Morris water maze (MWM) on Days 4 and 5. Analysis with repeated 2-way analysis of variance (ANOVA) indicated a significant effect of treatment on escape latency but no effect of timepoint or a timepoint \times treatment interaction. Post hoc analysis by Tukey's multiple comparisons test showed significant differences between the control and 6-OHDA-treated groups on the 4th and 5th days of training. * $p < 0.05$, ** $p < 0.01$. Data are mean \pm SEM, $n = 10$. (C) The number of platform crossings during the probe trial indicated that 6-OHDA-injected rats show a deficit in reference memory compared with controls with fewer numbers of platform crossings. (D) Percentage of time spent per quadrant during the probe test. Analysis with repeated 2-way ANOVA indicated a significant effect of treatment on quadrant preference but no effect of timepoint or a timepoint \times treatment interaction. Post hoc analysis by Šidák's multiple comparisons test showed a significant effect of treatment for this parameter. ** $p < 0.01$. Data are mean \pm SEM, $n = 10$. (E) Traces of swim trajectories in the MWM probe test. Control rats, but not 6-OHDA-injected rats, show clear preference for the target quadrant (red outline).

a marked increase in nitrotyrosine-positive cells within the frontal cortex and hippocampal regions compared with control rats (Figure S11E).

To further explore the timing of these events, we also examined changes in rats 1 week following injection of 6-OHDA. At this timepoint, there is no significant loss of TH +ve cells in the SN, although

there was a trend towards a reduction in cell number in the contralateral hemisphere of 6-OHDA rats relative to controls (Figure S12). Oxidative stress was found to be significantly elevated in the SN, but not other regions, 1 week after 6-OHDA injection (Figure S13). This may result from the close proximity of the SN and MFB injection site.

Taken together, these data may suggest that in the absence of an oxidative stress response, aSyn PFFs may not be sufficient to induce rapid and major neurodegenerative changes in the frontal cortex and the hippocampus, despite the presence of phosphorylated aSyn.

6-OHDA-injected rats exhibited deficits in hippocampal-dependent visuospatial learning and an asymmetric motor impairment

It is established that 6-OHDA induces balance and/or coordination disabilities [64, 65]. Here, the asymmetric cylinder test was used to detect motor asymmetry. We observed a unilateral motor deficit with a reduction in forepaw usage during the asymmetric cylinder task in rats injected with 6-OHDA compared with control rats (Figure 8A). It is well-known that motor dysfunction is largely correlated with neuronal loss in the SN. However, in aSyn PFF-injected rats, we found only a transient reduction in contralateral forepaw usage at 90 d.p.i. (Figure S14A) but not at 60 d.p.i. or 120 d.p.i. (data not shown). These results suggest that there was no severe impairment of motor function in the aSyn PFF-injected rats, most likely because there was no significant loss of neurons in the SN following injection of aSyn PFF into rat MFB.

Lastly, to understand whether the neurodegenerative changes we observed in frontal cortex and hippocampus in 6-OHDA-injected rats caused cognitive deficits, the MWM was used to assess visuospatial impairment [45] by adapting a protocol previously established for this purpose [46]. Three weeks following injection of 6-OHDA, rats displayed an impairment during the training phases of the MWM, and their escape latencies in comparison with control rats were significantly increased (Figure 8B). On Day 1, both control and 6-OHDA groups showed the same escape latency. However, as the training phase proceeded, it became evident that 6-OHDA-injected rats were impaired whereas the control rats had a reduced escape latency time demonstrating learning. Furthermore, by Day 3, both groups plateaued in their learning, with control groups having a shorter escape latency overall, compared with 6-OHDA-injected rats. In addition to the spatial training phase, the MWM also detects reference memory. 6-OHDA-injected rats demonstrated an impairment in reference memory shown by decreased performance in locating the previous position of the platform in the probe trial (Figure 8C,D). Although analysis of the swim distance showed a significant difference between control and 6-OHDA-injected animals (Figure S15), the swim trajectories showed that control, but not 6-OHDA-injected rats, showed an evident preference for the target quadrant, which despite 6-OHDA-injected rats showing reduced swim length and speed demonstrates cognitive impairment in the 6-OHDA-injected animals (Figure 8E).

In contrast, despite the presence of phosphorylated aSyn labelling in neurons in the brains of the aSyn PFF-injected rats, we did not observe any sustained differences in cognition between control and aSyn PFF groups. Rats underwent behavioural tests as previously described for 6-OHDA-injected rats to detect any impairments in visuospatial activity and motor function at 60, 90 and 120 d.p.i. We found no difference in any MWM parameters examined between control and aSyn PFF-injected groups at any of the time points investigated (data shown from 90 d.p.i. only in Figure S14B–D).

6-OHDA and aSyn-PFF-injected rats did not exhibit anxiety behaviour

Finally, to ensure that rats did not exhibit any anxiety, which could affect their behavioural outcomes, we used the open field task to monitor anxiety related behaviour. Neither control nor 6-OHDA rats exhibited anxiety behaviour (Figure S16B), in keeping with the findings reported by others [66]. aSyn PFF-injected rats and controls also did not demonstrate anxiety behaviour. All groups spent similar amounts of time in the open centre zone (inner zone) (Figure S16A,B). Next, we investigated the rodents' land-based locomotor activity. Although there was a slight reduction in the distance travelled, there was no overall significant difference between control and 6-OHDA-injected groups or control and PFF groups (Figure S16C,D). Trajectories of representative rats during the open field task are shown (Figure S16E,F).

DISCUSSION

It is commonly considered that a neurodegenerative cascade is initiated downstream of the accumulation of aggregated proteins, eventually leading to degeneration of synapses and neurons, behavioural and/or cognitive deficits. Neuroinflammation can occur throughout disease course. Our study showed that aSyn PFFs induced the progressive appearance of phosphorylated aSyn throughout several regions of brain that are consistent with the concept of aSyn spread. This is in agreement with numerous reports showing that intracerebral injections of aSyn PFFs induce aSyn propagation in mice and rats [28, 29, 31, 32, 49]. The phosphorylation and accumulation of aSyn can affect synapses and mitochondria and are detrimental to neuron health [67]. However, we find that neurodegenerative events associated with phosphorylated aSyn following aSyn PFF injection are relatively slow to emerge. Similar findings were recently reported by others [5]. In contrast, 6-OHDA injection into the MFB caused rapid and marked neuronal death in the SN. This was associated with oxidative/nitrative stress in connected brain regions from as early as 1 week post-injection. There is a strong association between oxidative stress and aSyn accumulation [16, 68, 69], and in-keeping with this, we found accumulations of phosphorylated aSyn and tau in the frontal cortex and hippocampus, in addition to perturbation of synaptic proteins. Our study strongly suggests that increased levels of

oxidative/nitrative stress as a result of neurotoxic insult rapidly progressed to neurodegeneration in distal brain regions. We propose that such oxidative stress responses could be an important factor in the rapid conversion of PD to PDD.

It is believed that dementia associated with synucleinopathies results from a loss of connectivity within neuronal circuits [70] through which aSyn can spread [70, 71]. The MFB has traditionally been considered an ideal injection site for modelling PD because of its key projections to areas commonly associated with PD including the ST and SN. Furthermore, the MFB also has afferent and efferent projections to regions associated with executive function and visuospatial impairment in PD. Findings from animal studies have demonstrated that the spread/propagation of aSyn and tau pathology is determined by neuroconnectivity and not proximity [14, 72]. Therefore, aSyn PFFs were injected into the MFB to allow investigation of the role of aSyn in contributing to cognitive deficits in rats. We demonstrated that intracerebral injections of aSyn PFF into the rat MFB triggered trans-neuronal spreading of aSyn as indicated by the accumulation of phosphorylated aSyn in connected regions [14, 31, 32, 57]. Similarly, phosphorylated aSyn was found in the frontal cortex and hippocampus following 6-OHDA injection into rat MFB. While the vast majority of studies target major terminal fields [28, 30, 32, 57], the MFB injections are directed towards fibre-mediated effects, and the results suggest that neural projections of the MFB can promote progressive regional neurodegeneration. However, we were unable to detect any accumulation of sarkosyl-insoluble aSyn in these models. While it is possible that our methods were not sufficiently sensitive to detect aSyn aggregates, or soluble replication-competent aSyn oligomers, these data raise the possibility that the progressive emergence of phosphorylated aSyn is secondary to downstream changes resulting from local effects of aSyn PFF or 6-OHDA, rather than being the result of aSyn spread.

Although the characteristic hallmarks of PD are LBs and LNs, around 80% of patients show coexistent AD-like pathology [59, 60, 73–76]. Cross-seeding of tau and aSyn has previously been demonstrated [27], and tau is closely linked with synaptic degeneration in dementia [58, 77]. We have used wild-type rats in this study, and these animals do not readily produce A β aggregates and so they would not be expected to produce any A β pathology even following aSyn PFF injection. Indeed, this has been recently reported by others [52]. Therefore, we investigated if tau phosphorylation was induced by 6-OHDA. Accordingly, we found an increase in tau phosphorylation in our 6-OHDA-injected rats compared with controls. We also found that pS404 tau immunoreactivity was higher in 6-OHDA rats compared with controls. The CA1 region of 6-OHDA-injected rats showed increased levels of pS404 tau immunoreactivity, predominantly in the somatodendritic region, which is reminiscent of tau changes during early tauopathy development [78].

The spreading/accumulation of pathological proteins is generally believed to be the first step in the neurodegenerative cascade. Exogenous aSyn PFFs can induce spread of aSyn over time but was not sufficient to induce phosphorylation of endogenous tau along the MFB pathway, at least during the timeframes examined here. This is

important because these results may suggest that spread of aSyn alone would result in slow conversion of PD into PDD. In contrast, the Parkinsonian mimetic 6-OHDA induced phosphorylation of both aSyn and some epitopes of tau in the frontal cortex and the hippocampus within 3 weeks. Although many reports show the oxidative stress-inducing properties of 6-OHDA [79, 80], the free radical properties of 6-OHDA are short-lived and are unlikely to fully explain the neurodegenerative events observed in the cortex and hippocampus. Indeed, there are increased levels not only of oxidative stress but also nitrative stress in the frontal cortex and the hippocampus.

Synaptic degeneration/neuronal loss is believed to result from the accumulation of pathological proteins as they spread along anatomical connections. We observed a specific loss of the post-synaptic protein PSD-95, but not of pre-synaptic proteins, in the frontal cortex after 6-OHDA injections, in addition to acute loss of SN neurons within 3 weeks. We do not believe that these effects are related to changes in phosphorylated tau because we observed significant increases in tau phosphorylation at Ser404 in hippocampal sub-fields but not in the frontal cortex. In contrast, we detected reduced PSD-95 amounts in the frontal cortex but not the hippocampus. However, we cannot rule out that tau-directed effects on synapses could be mediated by alterations in tau phosphorylation at other residues or other tau modifications. In addition, perhaps there are other functional changes in tau that were not examined here such as increased tau localisation at synapses. Some neurons along the MFB project to the frontal cortex, and our findings suggest that dying neurons in the SN release toxic substances, including oxidative/nitrative stress mediators that can affect post-synaptic densities in the frontal cortex. Pre-synaptic proteins were not affected, and it may be that these are more resilient to oxidative and nitrative stress under these conditions. For aSyn PFFs, we could not detect any loss of synaptic proteins up to 120 days after injection and neither was any significant oxidative/nitrative stress detected in the frontal cortex. However, there was some loss of SN neurons at 120 d.p.i., but not at earlier time points. Thus, oxidative/nitrative stress induced by substantial and rapid neuron loss may potentiate the spread and accumulation of pathological proteins within neural circuits, and therefore, we suggest that this could accelerate the conversion of PD to PDD.

This assertion is further supported by our behavioural tests in 6-OHDA rats. As a result of TH neuron loss, motor impairment was observed in the asymmetric cylinder test, in line with previous literature [65, 81–83]. In addition to motor deficits, we found impairments in spatial learning and reference memory in the 6-OHDA-injected group, in agreement with a previous report [84].

Taken together, our results demonstrate that (a) neurodegeneration resulting from pathological protein spread may be a slow process which resembles neurodegeneration in human patients; (b) although this process usually starts with spread/accumulation of pathological proteins, the onset of neurodegenerative processes in widespread brain regions can be accelerated by neuronal loss, including upon (c) increased levels of oxidative/nitrative stress related to dying neurons, whereas (d) a gradual process of neuronal loss, such as that resulting from protein aggregate spread, induced

minimal oxidative/nitrative stress and resulted in a slow progression of neurodegeneration. We therefore propose that future therapeutic interventions to slow or prevent the conversion of PD to PDD may be through the reduction of oxidative/nitrative stress.

ACKNOWLEDGEMENTS

We thank Alan Liu, Becky Stell, Rachel Wang, Joycelyn Xiao, Jessica Chu, Katherine Tang, Vesela Gesheva, Anna Sarika Varma, Matthew Peniket, Alvin Wong, Glenn Chang, Haydn Shiu, John Chu and Jeffery Lau for their technical support and assistance. We thank the late Professor Peter Davies (Feinstein Institute of Medical Research, NY, USA) for his kind gift of tau antibodies. We dedicate this manuscript to the memory of Professor John Trojanowski.

CONFLICT OF INTEREST

The authors declare no competing interests.

ETHICAL STATEMENT

All animal studies were approved by HKU and performed in accordance with the Committee on the use of Live animals in teaching and research (CULATR regulations), in which the guidelines of the National Centre for the Replacement, Refinement and Reduction of Animals in Research, UK, and NIH Guidelines for Survival Rodent Surgery, USA are followed. Post-mortem brain tissue was obtained from the London Neurodegenerative Diseases Brain Bank at King's College London (REC approval 18/WA/0206).

AUTHOR CONTRIBUTIONS

CCCP performed the experiments and analysed the results. MHS performed the additional 6-OHDA experiments and behavioural tests. KCL, JQT and VMYL synthesised and provided the PFFs and 81A antibody. They also gave intellectual advice on this study. RCCC and WN designed the study, participated in discussion and supervised the whole study. CCCP, WN and RCCC wrote and revised the manuscript. All authors read and approved the final manuscript.

DATA AVAILABILITY STATEMENT

The data that support the findings of this study are available from the corresponding author upon reasonable request.

ORCID

Wendy Noble  <https://orcid.org/0000-0002-7898-4295>

Raymond C. C. Chang  <https://orcid.org/0000-0001-8538-7993>

REFERENCES

1. Clinton LK, Blurton-Jones M, Myczek K, Trojanowski JQ, LaFerla FM. Synergistic Interactions between Abeta, tau, and alpha-synuclein: acceleration of neuropathology and cognitive decline. *J Neurosci*. 2010;30(21):7281-7289. doi:10.1523/JNEUROSCI.0490-10.2010
2. Masliah E, Rockenstein E, Veinbergs I, et al. beta-amyloid peptides enhance alpha-synuclein accumulation and neuronal deficits in a transgenic mouse model linking Alzheimer's disease and Parkinson's

- disease. *Proc Natl Acad Sci U S A*. 2001;98(21):12245-12250. doi:10.1073/pnas.211412398
3. Irwin DJ, Hurtig HI. The contribution of tau, amyloid-beta and alpha-synuclein pathology to dementia in Lewy body disorders. *J Alzheimers Dis Parkinsonism*. 2018;8(04):444. doi:10.4172/2161-0460.1000444
4. Irwin DJ, White MT, Toledo JB, et al. Neuropathologic substrates of Parkinson disease dementia. *Ann Neurol*. 2012;72(4):587-598. doi:10.1002/ana.23659
5. Garcia P, Jurgens-Wemheuer W, Uriarte Huarte O, et al. Neurodegeneration and neuroinflammation are linked, but independent of alpha-synuclein inclusions, in a seeding/spreading mouse model of Parkinson's disease. *Glia*. 2022;70(5):935-960. doi:10.1002/glia.24149
6. Peng C, Gathagan RJ, Covell DJ, et al. Cellular milieu imparts distinct pathological alpha-synuclein strains in alpha-synucleinopathies. *Nature*. 2018;557(7706):558-563. doi:10.1038/s41586-018-0104-4
7. Peng C, Gathagan RJ, Lee VM. Distinct alpha-Synuclein strains and implications for heterogeneity among alpha-Synucleinopathies. *Neurobiol Dis*. 2018;109(Pt B):209-218. doi:10.1016/j.nbd.2017.07.018
8. Hely MA, Reid WG, Adena MA, Halliday GM, Morris JG. The Sydney multicenter study of Parkinson's disease: the inevitability of dementia at 20 years. *Mov Disord*. 2008;23(6):837-844. doi:10.1002/mds.21956
9. Aarsland D, Creese B, Politis M, et al. Cognitive decline in Parkinson disease. *Nat Rev Neurol*. 2017;13(4):217-231. doi:10.1038/nrneurol.2017.27
10. Serrano-Pozo A, Frosch MP, Masliah E, Hyman BT. Neuropathological alterations in Alzheimer disease. *Cold Spring Harb Perspect Med*. 2011;1(1):a006189. doi:10.1101/cshperspect.a006189
11. Liu AKL, Chau TW, Lim EJ, et al. Hippocampal CA2 Lewy pathology is associated with cholinergic degeneration in Parkinson's disease with cognitive decline. *Acta Neuropathol Commun*. 2019;7(1):61. doi:10.1186/s40478-019-0717-3
12. Pang CC, Kiecker C, O'Brien JT, Noble W, Chang RC. Ammon's Horn 2 (CA2) of the hippocampus: a long-known region with a new potential role in neurodegeneration. *Neuroscientist*. 2019;25(2):167-180. doi:10.1177/1073858418778747
13. Peng C, Trojanowski JQ, Lee VM. Protein transmission in neurodegenerative disease. *Nat Rev Neurol*. 2020;16(4):199-212. doi:10.1038/s41582-020-0333-7
14. Henderson MX, Cornblath EJ, Darwich A, et al. Spread of alpha-synuclein pathology through the brain connectome is modulated by selective vulnerability and predicted by network analysis. *Nat Neurosci*. 2019;22(8):1248-1257. doi:10.1038/s41593-019-0457-5
15. Singh B, Covelo A, Martell-Martinez H, et al. Tau is required for progressive synaptic and memory deficits in a transgenic mouse model of alpha-synucleinopathy. *Acta Neuropathol*. 2019;138(4):551-574. doi:10.1007/s00401-019-02032-w
16. Musgrove RE, Helwig M, Bae EJ, et al. Oxidative stress in vagal neurons promotes parkinsonian pathology and intercellular alpha-synuclein transfer. *J Clin Invest*. 2019;130(9):3738-3753. doi:10.1172/JCI127330
17. Luna E, Decker SC, Riddle DM, et al. Differential alpha-synuclein expression contributes to selective vulnerability of hippocampal neuron subpopulations to fibril-induced toxicity. *Acta Neuropathol*. 2018;135(6):855-875. doi:10.1007/s00401-018-1829-8
18. Puspita L, Chung SY, Shim JW. Oxidative stress and cellular pathologies in Parkinson's disease. *Mol Brain*. 2017;10(1):53. doi:10.1186/s13041-017-0340-9
19. Jenner P. Oxidative stress in Parkinson's disease. *Ann Neurol*. 2003;53(Suppl 3):S26-S36; discussion S-8. doi:10.1002/ana.10483
20. Yoritaka A, Hattori N, Uchida K, Tanaka M, Stadtman ER, Mizuno Y. Immunohistochemical detection of 4-hydroxynonenal protein

- adducts in Parkinson disease. *Proc Natl Acad Sci U S A*. 1996;93(7):2696-2701. doi:10.1073/pnas.93.7.2696
21. Alam ZI, Jenner A, Daniel SE, et al. Oxidative DNA damage in the parkinsonian brain: an apparent selective increase in 8-hydroxyguanine levels in substantia nigra. *J Neurochem*. 1997;69(3):1196-1203. doi:10.1046/j.1471-4159.1997.69031196.x
 22. Zhang J, Perry G, Smith MA, et al. Parkinson's disease is associated with oxidative damage to cytoplasmic DNA and RNA in substantia nigra neurons. *Am J Pathol*. 1999;154(5):1423-1429. doi:10.1016/S0002-9440(10)65396-5
 23. Good PF, Hsu A, Werner P, Perl DP, Olanow CW. Protein nitration in Parkinson's disease. *J Neurobiol*. 1998;30(4):338-342. doi:10.1002/9781118133120.ch4
 24. Duda JE, Giasson BI, Chen Q, et al. Widespread nitration of pathological inclusions in neurodegenerative synucleinopathies. *Am J Pathol*. 2000;157(5):1439-1445. doi:10.1016/S0002-9440(10)64781-5
 25. Hwang O. Role of oxidative stress in Parkinson's disease. *Exp Neurol*. 2013;22(1):11-17. doi:10.5607/en.2013.22.1.11
 26. Dias V, Junn E, Mouradian MM. The role of oxidative stress in Parkinson's disease. *J Parkinsons Dis*. 2013;3(4):461-491. doi:10.3233/JPD-130230
 27. Castillo-Carranza DL, Guerrero-Munoz MJ, Sengupta U, Gerson JE, Kaye R. alpha-Synuclein oligomers induce a unique toxic tau strain. *Biol Psychiatry*. 2018;84(7):499-508. doi:10.1016/j.biopsych.2017.12.018
 28. Paumier KL, Luk KC, Manfredsson FP, et al. Intrastriatal injection of pre-formed mouse alpha-synuclein fibrils into rats triggers alpha-synuclein pathology and bilateral nigrostriatal degeneration. *Neurobiol Dis*. 2015;82:185-199. doi:10.1016/j.nbd.2015.06.003
 29. Kim S, Kwon SH, Kam TI, et al. Transneuronal propagation of pathologic alpha-synuclein from the gut to the brain models Parkinson's disease. *Neuron*. 2019;103(4):627-641 e7. doi:10.1016/j.neuron.2019.05.035
 30. Patterson JR, Duffy MF, Kemp CJ, et al. Time course and magnitude of alpha-synuclein inclusion formation and nigrostriatal degeneration in the rat model of synucleinopathy triggered by intrastriatal alpha-synuclein preformed fibrils. *Neurobiol Dis*. 2019;130:104525. doi:10.1016/j.nbd.2019.104525
 31. Rey NL, George S, Steiner JA, et al. Spread of aggregates after olfactory bulb injection of alpha-synuclein fibrils is associated with early neuronal loss and is reduced long term. *Acta Neuropathol*. 2018;135(1):65-83. doi:10.1007/s00401-017-1792-9
 32. Luk KC, Kehm V, Carroll J, et al. Pathological alpha-synuclein transmission initiates Parkinson-like neurodegeneration in nontransgenic mice. *Science*. 2012;338(6109):949-953. doi:10.1126/science.1227157
 33. Shah A, Han P, Wong MY, Chang RC, Legido-Quigley C. Palmitate and stearate are increased in the plasma in a 6-OHDA model of Parkinson's disease. *Metabolites*. 2019;9(2). doi:10.3390/metabo9020031
 34. Nieuwenhuys R, Geeraedts LM, Veening JG. The medial forebrain bundle of the rat. I General Introduction. *J Comp Neurol*. 1982;206(1):49-81. doi:10.1002/cne.902060106
 35. McMullen NT, Almli CR. Cell types within the medial forebrain bundle: a Golgi study of preoptic and hypothalamic neurons in the rat. *Am J Anat*. 1981;161(3):323-340. doi:10.1002/aja.1001610306
 36. Shiosaka S, Tohyama M, Takagi H, et al. Ascending and descending components of the medial forebrain bundle in the rat as demonstrated by the horseradish peroxidase-blue reaction. I Forebrain and Upper Brain Stem. *Exp Brain Res*. 1980;39(4):377-388. doi:10.1007/BF00239302
 37. Veening JG, Swanson LW, Cowan WM, Nieuwenhuys R, Geeraedts LM. The medial forebrain bundle of the rat. II. An autoradiographic study of the topography of the major descending and ascending components. *J Comp Neurol*. 1982;206(1):82-108. doi:10.1002/cne.902060107
 38. Polinski NK, Volpicelli-Daley LA, Sortwell CE, et al. Best practices for generating and using alpha-synuclein pre-formed fibrils to model Parkinson's disease in rodents. *J Parkinsons Dis*. 2018;8(2):303-322. doi:10.3233/JPD-171248
 39. Zhang B, Kehm V, Gathagan R, et al. Stereotaxic targeting of alpha-synuclein pathology in mouse brain using preformed fibrils. *Methods Mol Biol*. 2019;1948:45-57. doi:10.1007/978-1-4939-9124-2_5
 40. Torres EM, Lane EL, Heuer A, Smith GA, Murphy E, Dunnett SB. Increased efficacy of the 6-hydroxydopamine lesion of the median forebrain bundle in small rats, by modification of the stereotaxic coordinates. *J Neurosci Methods*. 2011;200(1):29-35. doi:10.1016/j.jneumeth.2011.06.012
 41. Markel AL, Galaktionov Yu K, Efimov VM. Factor analysis of rat behavior in an open field test. *Neurosci Behav Physiol*. 1989;19(4):279-286. doi:10.1007/BF01236015
 42. Kollensperger M, Stampfer-Kountchev M, Seppi K, et al. Progression of dysautonomia in multiple system atrophy: a prospective study of self-perceived impairment. *Eur J Neurol*. 2007;14(1):66-72. doi:10.1111/j.1468-1331.2006.01554.x
 43. Jerussi TP, Glick SD. Apomorphine-induced rotation in normal rats and interaction with unilateral caudate lesions. *Psychopharmacologia*. 1975;40(4):329-334. doi:10.1007/BF00421471
 44. Majlessi N, Choopani S, Kamalinejad M, Azizi Z. Amelioration of amyloid beta-induced cognitive deficits by Zataria multiflora Boiss. essential oil in a rat model of Alzheimer's disease. *CNS Neurosci Ther*. 2012;18(4):295-301. doi:10.1111/j.1755-5949.2011.00237.x
 45. Vorhees CV, Williams MT. Morris water maze: procedures for assessing spatial and related forms of learning and memory. *Nat Protoc*. 2006;1(2):848-858. doi:10.1038/nprot.2006.116
 46. You R, Liu Y, Chang RC. A behavioral test battery for the repeated assessment of motor skills, mood, and cognition in mice. *J Vis Exp*. 2019;(145):e58973. doi:10.3791/58973
 47. Ho YS, Yang X, Yeung SC, et al. Cigarette smoking accelerated brain aging and induced pre-Alzheimer-like neuropathology in rats. *PLoS ONE*. 2012;7(5):e36752. doi:10.1371/journal.pone.0036752
 48. Nolan M, Troakes C, King A, Bodi I, Al-Sarraj S. Control tissue in brain banking: the importance of thorough neuropathological assessment. *J Neural Transm (Vienna)*. 2015;122(7):949-956. doi:10.1007/s00702-015-1376-6
 49. Okuzumi A, Kurosawa M, Hatano T, et al. Rapid dissemination of alpha-synuclein seeds through neural circuits in an in-vivo prion-like seeding experiment. *Acta Neuropathol Commun*. 2018;6(1):96. doi:10.1186/s40478-018-0587-0
 50. Moussaud S, Jones DR, Moussaud-Lamodièrre EL, Delenclos M, Ross OA, McLean PJ. Alpha-synuclein and tau: teammates in neurodegeneration? *Mol Neurodegener*. 2014;9(1):43. doi:10.1186/1750-1326-9-43
 51. Vasili E, Dominguez-Meijide A, Outeiro TF. Spreading of alpha-synuclein and tau: a systematic comparison of the mechanisms involved. *Front Mol Neurosci*. 2019;12:107. doi:10.3389/fnmol.2019.00107
 52. Bassil F, Brown HJ, Pattabhiraman S, et al. Amyloid-beta (Aβ) plaques promote seeding and spreading of alpha-synuclein and tau in a mouse model of Lewy body disorders with Aβ pathology. *Neuron*. 2020;105(2):260-275 e6. doi:10.1016/j.neuron.2019.10.010
 53. Waxman EA, Giasson BI. Induction of intracellular tau aggregation is promoted by alpha-synuclein seeds and provides novel insights into the hyperphosphorylation of tau. *J Neurosci*. 2011;31(21):7604-7618. doi:10.1523/JNEUROSCI.0297-11.2011
 54. Giasson BI, Forman MS, Higuchi M, et al. Initiation and synergistic fibrillization of tau and alpha-synuclein. *Science*. 2003;300(5619):636-640. doi:10.1126/science.1082324

55. Wu Q, Takano H, Riddle DM, Trojanowski JQ, Coulter DA, Lee VM. alpha-Synuclein (alphaSyn) preformed fibrils induce endogenous alphasyn aggregation, compromise synaptic activity and enhance synapse loss in cultured excitatory hippocampal neurons. *J Neurosci*. 2019;39(26):5080-5094. doi:10.1523/JNEUROSCI.0060-19.2019
56. Duffy MF, Collier TJ, Patterson JR, et al. Lewy body-like alpha-synuclein inclusions trigger reactive microgliosis prior to nigral degeneration. *J Neuroinflammation*. 2018;15(1):129. doi:10.1186/s12974-018-1171-z
57. Abdelmotilib H, Maltbie T, Delic V, et al. alpha-Synuclein fibril-induced inclusion spread in rats and mice correlates with dopaminergic neurodegeneration. *Neurobiol Dis*. 2017;105:84-98. doi:10.1016/j.nbd.2017.05.014
58. Perez-Nievas BG, Stein TD, Tai HC, et al. Dissecting phenotypic traits linked to human resilience to Alzheimer's pathology. *Brain*. 2013;136(8):2510-2526. doi:10.1093/brain/awt171
59. Irwin DJ, Lee VM, Trojanowski JQ. Parkinson's disease dementia: convergence of alpha-synuclein, tau and amyloid-beta pathologies. *Nat Rev Neurosci*. 2013;14(9):626-636. doi:10.1038/nrn3549
60. Guo T, Noble W, Hanger DP. Roles of tau protein in health and disease. *Acta Neuropathol*. 2017;133(5):665-704. doi:10.1007/s00401-017-1707-9
61. Hanger DP, Byers HL, Wray S, et al. Novel phosphorylation sites in tau from Alzheimer brain support a role for casein kinase 1 in disease pathogenesis. *J Biol Chem*. 2007;282(32):23645-23654. doi:10.1074/jbc.M703269200
62. Sri S, Pegasiou CM, Cave CA, et al. Emergence of synaptic and cognitive impairment in a mature-onset APP mouse model of Alzheimer's disease. *Acta Neuropathol Commun*. 2019;7(1):25. doi:10.1186/s40478-019-0670-1
63. Orock A, Logan S, Deak F. Age-related cognitive impairment: role of reduced synaptobrevin-2 levels in memory and synaptic plasticity deficits. *J Gerontol A Biol Sci Med Sci*. 2019;75(9):1624-1632. doi:10.1093/gerona/glz013
64. Glajch KE, Fleming SM, Surmeier DJ, Osten P. Sensorimotor assessment of the unilateral 6-hydroxydopamine mouse model of Parkinson's disease. *Behav Brain Res*. 2012;230(2):309-316. doi:10.1016/j.bbr.2011.12.007
65. Decressac M, Mattsson B, Bjorklund A. Comparison of the behavioural and histological characteristics of the 6-OHDA and alpha-synuclein rat models of Parkinson's disease. *Exp Neurol*. 2012;235(1):306-315. doi:10.1016/j.expneurol.2012.02.012
66. Carvalho MM, Campos FL, Coimbra B, et al. Behavioral characterization of the 6-hydroxydopamine model of Parkinson's disease and pharmacological rescuing of non-motor deficits. *Mol Neurodegener*. 2013;8(1):14. doi:10.1186/1750-1326-8-14
67. Ganjam GK, Bolte K, Matschke LA, et al. Mitochondrial damage by alpha-synuclein causes cell death in human dopaminergic neurons. *Cell Death Dis*. 2019;10(11):865. doi:10.1038/s41419-019-2091-2
68. Esteves AR, Arduino DM, Swerdlow RH, Oliveira CR, Cardoso SM. Oxidative stress involvement in alpha-synuclein oligomerization in Parkinson's disease cybrids. *Antioxid Redox Signal*. 2009;11(3):439-448. doi:10.1089/ars.2008.2247
69. Gallegos S, Pacheco C, Peters C, Opazo CM, Aguayo LG. Features of alpha-synuclein that could explain the progression and irreversibility of Parkinson's disease. *Front Neurosci*. 2015;9:59. doi:10.3389/fnins.2015.00059
70. Braak H, Del Tredici K, Rub U, de Vos RA, Jansen Steur EN, Braak E. Staging of brain pathology related to sporadic Parkinson's disease. *Neurobiol Aging*. 2003;24(2):197-211. doi:10.1016/S0197-4580(02)00065-9
71. Braak H, Ghebremedhin E, Rub U, Bratzke H, Del Tredici K. Stages in the development of Parkinson's disease-related pathology. *Cell Tissue Res*. 2004;318(1):121-134. doi:10.1007/s00441-004-0956-9
72. Ahmed Z, Cooper J, Murray TK, et al. A novel in vivo model of tau propagation with rapid and progressive neurofibrillary tangle pathology: the pattern of spread is determined by connectivity, not proximity. *Acta Neuropathol*. 2014;127(5):667-683. doi:10.1007/s00401-014-1254-6
73. Colom-Cadena M, Gelpi E, Charif S, et al. Confluence of alpha-synuclein, tau, and beta-amyloid pathologies in dementia with Lewy bodies. *J Neuropathol Exp Neurol*. 2013;72(12):1203-1212. doi:10.1097/NEN.000000000000018
74. Delenclos M, Moussaud S, McLean PJ. Untangling a role for tau in synucleinopathies. *Biol Psychiatry*. 2015;78(10):666-667. doi:10.1016/j.biopsych.2015.08.020
75. Sengupta U, Guerrero-Munoz MJ, Castillo-Carranza DL, et al. Pathological interface between oligomeric alpha-synuclein and tau in synucleinopathies. *Biol Psychiatry*. 2015;78(10):672-683. doi:10.1016/j.biopsych.2014.12.019
76. Spires-Jones TL, Attems J, Thal DR. Interactions of pathological proteins in neurodegenerative diseases. *Acta Neuropathol*. 2017;134(2):187-205. doi:10.1007/s00401-017-1709-7
77. Ittner LM, Ke YD, Delerue F, et al. Dendritic function of tau mediates amyloid-beta toxicity in Alzheimer's disease mouse models. *Cell*. 2010;142(3):387-397. doi:10.1016/j.cell.2010.06.036
78. Noble W, Hanger DP, Miller CC, Lovestone S. The importance of tau phosphorylation for neurodegenerative diseases. *Front Neurol*. 2013;4:83. doi:10.3389/fneur.2013.00083
79. Hernandez-Baltazar D, Zavala-Flores LM, Villanueva-Olivo A. The 6-hydroxydopamine model and parkinsonian pathophysiology: Novel findings in an older model. *Neurologia*. 2017;32(8):533-539. doi:10.1016/j.nrleng.2015.06.019
80. Ferger B, Rose S, Jenner A, Halliwell B, Jenner P. 6-hydroxydopamine increases hydroxyl free radical production and DNA damage in rat striatum. *Neuroreport*. 2001;12(6):1155-1159. doi:10.1097/00001756-200105080-00021
81. Alvarez-Fischer D, Henze C, Strenzke C, et al. Characterization of the striatal 6-OHDA model of Parkinson's disease in wild type and alpha-synuclein-deleted mice. *Exp Neurol*. 2008;210(1):182-193. doi:10.1016/j.expneurol.2007.10.012
82. Beal MF. Experimental models of Parkinson's disease. *Nat Rev Neurosci*. 2001;2(5):325-334. doi:10.1038/35072550
83. Heuer A, Smith GA, Dunnett SB. Comparison of 6-hydroxydopamine lesions of the substantia nigra and the medial forebrain bundle on a lateralised choice reaction time task in mice. *Eur J Neurosci*. 2013;37(2):294-302. doi:10.1111/ejn.12036
84. Ma Y, Zhan M, OuYang L, et al. The effects of unilateral 6-OHDA lesion in medial forebrain bundle on the motor, cognitive dysfunctions and vulnerability of different striatal interneuron types in rats. *Behav Brain Res*. 2014;266:37-45. doi:10.1016/j.bbr.2014.02.039

SUPPORTING INFORMATION

Additional supporting information can be found online in the Supporting Information section at the end of this article.

How to cite this article: Pang CCC, Sørensen MH, Lee K, et al. Investigating key factors underlying neurodegeneration linked to alpha-synuclein spread. *Neuropathol Appl Neurobiol*. 2022; 48(6):e12829. doi:10.1111/nan.12829